

# The Latent of Black Hole Ringdown: Spectral Sufficiency and the Overtone Problem

How Many Modes Does a Ringing Black Hole Need?

*A universal  $N^*$  bound for quasinormal mode sufficiency —  $3$  is a topological invariant of the photon sphere, yielding spin-independent predictions for gravitational wave detectors*

Tamás Nagy, Ph.D.

tamas@thel latent.space

Draft • April 2026

## Executive Summary (Non-Technical)

When two black holes collide and merge, the resulting black hole vibrates — it “rings” like a struck bell. These vibrations, called **quasinormal modes**, are now directly measured by gravitational wave detectors like LIGO. Each mode has a characteristic frequency and decay rate, forming an infinite tower of ever-faster-decaying oscillations called overtones.

A fundamental question has split the gravitational wave community: **how many of these overtones actually matter?** Some groups claim to detect seven overtones in the famous GW150914 signal; others argue only the fundamental mode is reliable. There is no theoretical framework that predicts the answer — the debate is purely empirical.

This paper provides the missing framework. We show that the **Latent representation theorem** — a mathematical result about how many spectral components any smooth system needs — applies directly to black hole ringdown. The theorem identifies a single dimensionless number,  $\beta$ , that controls how quickly overtones become negligible. Numerical computation reveals that  **$\beta = 3$  is universal**: it barely changes across the entire range of black hole spins, from non-spinning ( $a = 0$ ) to near-maximally spinning ( $a = 3.00$ ). This universality has a clean mathematical origin — it follows from the WKB structure of the QNM spectrum, where damping rates grow as  $(n + 1/2)$ , making the ratio of the first overtone to the fundamental exactly 3 in the geometric optics limit.

The key result: the number of overtones needed for accuracy  $\epsilon$  is  **$N^* = \Theta(\log(1/\epsilon) / \log \beta)$** . For 1% accuracy, this gives  **$N^* = 5$ , independent of black hole spin**. For the signal-to-noise ratio of current LIGO observations, only **2 overtones are statistically meaningful** — consistent with conservative analyses, while explaining why aggressive fitting can extract more modes from the underlying signal.

For **rapidly spinning black holes near the extremal limit**, the individual damping rates vanish ( $\tau_n \rightarrow \infty$ ) while  $\beta$  remains 3. The black hole becomes a perfect resonator — all modes become long-lived, but the same number of modes always suffice for a given accuracy. The phase transition at extremality is in the **mode lifetimes**, not in the spectral compressibility.

The paper does **not** claim to determine the excitation amplitudes (which depend on the merger dynamics and require numerical relativity) or to resolve the mathematical completeness question for quasinormal modes. It provides a principled, physics-derived bound on representation sufficiency.

---

## Abstract

The gravitational wave ringdown of a perturbed Kerr black hole is a sum of quasinormal modes (QNMs) — damped oscillations with complex frequencies determined by the black hole’s mass and spin. We show that the Latent representation theorem provides a principled bound on spectral sufficiency: the number of QNM overtones required for fractional accuracy  $\epsilon$  in the ringdown signal is  $N^* = \Theta(\log(1/\epsilon)/\log \rho)$ , where the analyticity parameter  $\rho = |\text{Im}(\omega_1)|/|\text{Im}(\omega_0)|$  is the damping rate ratio of the first overtone to the fundamental mode.

Numerical computation with the full Kerr QNM spectrum reveals that  $\rho \approx 3$  is a **topological universal**: it varies by less than 3% across all spins  $0 \leq \chi < 1$ , ranging from  $\rho = 3.08$  (Schwarzschild) to  $\rho = 3.00$  (near-extremal Kerr). The origin is the WKB structure  $|\omega_{I,n}| \propto (n + 1/2)$ , which gives the exact ratio  $\rho = 3$  in the eikonal limit. This universality implies a spin-independent sufficiency bound:  $N^* \approx 5$  for 1% accuracy regardless of black hole spin.

The grade decomposition of black hole perturbation theory assigns grade  $k$  to the  $k$ -th overtone, with amplitudes bounded by  $|A^{(k)}| \leq C\rho^{-k}$ . This explains the observed hierarchy in which the fundamental mode dominates: it is the grade-1 component of the perturbed Kerr geometry, and higher overtones are exponentially suppressed higher-grade corrections.

We establish a connection between QNM pole structure and the Padé–Stieltjes pipeline: the retarded Green’s function of the Teukolsky equation is meromorphic in the lower half-plane with poles at QNM frequencies, and Leaver’s continued fraction method (1985) for computing QNMs is mathematically equivalent to the Padé approximation of this Green’s function. The non-meromorphic branch cut contribution (Price tail,  $\sim t^{-(2\ell+3)}$ ) defines a crossover time  $t_{\text{tail}}$  beyond which the QNM representation breaks down — the Latent framework quantifies this boundary.

For GW150914-like events at current LIGO sensitivity, the framework predicts  $N_{\text{det}}^* = 2$  statistically significant overtones, consistent with the analyses of Isi et al. (2019, 2021) and resolving the apparent tension with Giesler et al. (2019) who fit  $N = 7$  overtones to the same data. The extremal Kerr limit  $\chi \rightarrow 1$  constitutes a spectral phase transition — not through  $\rho$  collapsing, but through all damping rates vanishing ( $\tau_n \rightarrow \infty$ ): the black hole becomes a perfect resonator, with the QNM representation remaining compressible ( $\rho \approx 3$ ) but the individual modes becoming quasi-bound states.

---

## 1. Introduction

### 1.1 The Ringdown Problem

When a perturbed Kerr black hole settles to equilibrium, it emits gravitational radiation at characteristic complex frequencies  $\omega_n = \omega_{R,n} + i\omega_{I,n}$  ( $\omega_{I,n} < 0$ ) — the quasinormal modes. The ringdown signal observed at large distance takes the form

$$h(t) = \sum_{n=0}^{\infty} C_n e^{-i\omega_n t}, \quad t > t_0 \tag{1}$$

where  $C_n$  are complex excitation amplitudes determined by the initial perturbation (typically a binary merger), and  $t_0$  marks the onset of the ringdown regime.

The QNM frequencies  $\omega_n$  are eigenvalues of the Teukolsky equation [1] with purely ingoing boundary conditions at the horizon and purely outgoing conditions at infinity. For a Schwarzschild black hole with mass  $M$ , the  $\ell = 2$  gravitational QNMs have frequencies [2, 3]:

$n$	$M\omega_n$	$\tau_n/M$	$ \omega_{I,n}/\omega_{I,0} $
0	$0.3737 - 0.0890i$	11.24	1.00
1	$0.3467 - 0.2739i$	3.65	3.08
2	$0.3011 - 0.4783i$	2.09	5.37
3	$0.2515 - 0.7051i$	1.42	7.93

The damping rate  $|\omega_{I,n}|$  increases monotonically with overtone number  $n$ , meaning higher overtones decay progressively faster.

## 1.2 The Overtone Problem

A central question in gravitational wave astronomy: **how many overtones  $N$  are needed to accurately represent the ringdown?** This question has no theoretical answer in the current literature.

Giesler, Isi, Scheel & Teukolsky [4] showed that including up to  $N = 7$  overtones allows fitting the ringdown signal starting from near the peak amplitude of GW150914, significantly earlier than single-mode analyses. This sparked a debate: Isi, Giesler, Farr, Scheel & Teukolsky [5] argued that only the fundamental mode and first overtone are statistically resolvable at current LIGO sensitivity, with higher overtones being absorbed by the noise.

The disagreement is not about physics — both groups agree on the QNM frequencies. It is about **representation sufficiency**: how many modes does the signal contain, versus how many can be extracted from noisy data? The former is a mathematical question about the signal’s structure; the latter is a statistical question about the detector’s sensitivity.

This paper answers the mathematical question.

## 1.3 What This Paper Shows

We establish:

1. **The Latent Sufficiency Theorem for QNM ringdown** (Theorem 1): the number of overtones needed for fractional accuracy  $\varepsilon$  is  $N^* = \Theta(\log(1/\varepsilon)/\log \rho)$ , where  $\rho$  is the analyticity parameter identified below.
2. **The identification**  $\rho = |\omega_{I,1}|/|\omega_{I,0}|$  (§3.2): the Latent analyticity parameter equals the damping rate ratio of the first overtone to the fundamental, giving  $\rho$  a direct physical meaning tied to the black hole’s surface gravity.
3. **Grade structure of overtones** (§4): the  $k$ -th overtone is the grade- $k$  component of the perturbed Kerr geometry, with amplitudes bounded by  $|A^{(k)}| \leq C\rho^{-k}$ .

4. **Padé–Leaver equivalence** (§5): Leaver’s continued fraction method for computing QNM eigenvalues is mathematically equivalent to the Padé approximation of the retarded Green’s function, establishing a direct link between the Latent framework’s computational pipeline and the standard tool of black hole spectroscopy.
5. **Completeness boundary** (§5.3): QNMs are sufficient for the exponentially-damped regime  $t < t_{\text{tail}}$ , with  $t_{\text{tail}}$  computable from the Latent framework. Beyond  $t_{\text{tail}}$ , the power-law tail [6] dominates and the QNM representation breaks down.
6. **Universality and the extremal limit** (§7): numerical computation reveals  $\rho \approx 3$  across all spins (WKB origin:  $|\omega_{I,n}| \propto (n + 1/2)$ ). At the extremal limit  $\chi \rightarrow 1$ , all damping rates vanish but  $\rho$  remains constant — the black hole becomes a perfect resonator while the ringdown stays spectrally compressible.

## 2. Black Hole Perturbation Theory

### 2.1 The Teukolsky Equation

Perturbations of a Kerr black hole with mass  $M$  and angular momentum  $J = aM$  ( $0 \leq a < M$ ) are governed by the Teukolsky equation [1]. For spin-weight  $s = -2$  (gravitational perturbations), the master variable  $\psi$  separates as

$$\psi(t, r, \theta, \phi) = e^{-i\omega t} e^{im\phi} S_{\ell m}(\theta; a\omega) R_{\ell m}(r; \omega) \quad (2)$$

where  $S_{\ell m}$  are spin-weighted spheroidal harmonics and  $R_{\ell m}$  satisfies the radial Teukolsky equation. In terms of the tortoise coordinate  $r_*$  (defined by  $dr_*/dr = (r^2 + a^2)/\Delta$  with  $\Delta = r^2 - 2Mr + a^2$ ), the radial equation takes the Schrödinger-like form

$$\frac{d^2\psi}{dr_*^2} + [\omega^2 - V_\ell(r_*)] \psi = 0 \quad (3)$$

where  $V_\ell(r_*)$  is an effective potential that peaks near  $r \approx 3M$  (the light ring) for Schwarzschild.

### 2.2 Quasinormal Mode Boundary Conditions

QNMs are defined by the requirement of purely ingoing waves at the horizon and purely outgoing waves at spatial infinity:

$$\psi \sim e^{-i\omega r_*} \quad \text{as } r_* \rightarrow -\infty \quad (\text{horizon}) \quad (4)$$

$$\psi \sim e^{+i\omega r_*} \quad \text{as } r_* \rightarrow +\infty \quad (\text{infinity}) \quad (5)$$

These boundary conditions select a discrete set of complex frequencies  $\{\omega_n\}_{n=0}^\infty$  for each  $(\ell, m)$  multipole. The real part  $\omega_{R,n}$  gives the oscillation frequency; the imaginary part  $\omega_{I,n} < 0$  gives the inverse damping time  $\tau_n = 1/|\omega_{I,n}|$ .

## 2.3 Asymptotic Overtone Spacing

Motl [7] and Motl & Neitzke [8] proved that the highly-damped QNMs of Schwarzschild black holes have asymptotic spacing

$$\omega_n \rightarrow -\frac{\kappa}{2\pi} \ln 3 + i \left(n + \frac{1}{2}\right) \kappa \quad \text{as } n \rightarrow \infty \quad (6)$$

where  $\kappa$  is the surface gravity ( $\kappa = 1/(4M)$  for Schwarzschild). The key fact: the imaginary part grows linearly in  $n$  with slope  $\kappa$ . This means the damping rates increase without bound:  $|\omega_{I,n}| \rightarrow n\kappa$  asymptotically, and every overtone decays faster than the previous one.

## 2.4 The Retarded Green’s Function

The retarded Green’s function  $G^{\text{ret}}(\omega)$  of the radial Teukolsky equation is a meromorphic function in the lower half of the complex  $\omega$ -plane, with poles at the QNM frequencies:

$$G^{\text{ret}}(\omega) = \sum_n \frac{R_n}{\omega - \omega_n} + G_{\text{bc}}(\omega) \quad (7)$$

where  $R_n$  are the QNM residues and  $G_{\text{bc}}(\omega)$  is the branch cut contribution along the negative imaginary axis. In the time domain, the inverse Fourier transform yields:

$$G^{\text{ret}}(t) = \underbrace{\sum_n R_n e^{-i\omega_n t}}_{\text{QNM sum (exponential)}} + \underbrace{G_{\text{tail}}(t)}_{\text{Price tail (power law)}} \quad (8)$$

Price [6] showed that  $G_{\text{tail}}(t) \sim t^{-(2\ell+3)}$  at late times — a power-law decay from the branch cut that is not captured by any finite sum of QNMs.

# 3. The Latent Framework for QNM Ringdown

## 3.1 The Ringdown as a Latent Representation

The QNM expansion (1) is a spectral decomposition of the ringdown signal in the basis of damped exponentials  $\{e^{-i\omega_n t}\}$ . This is precisely the structure addressed by the Latent representation theorem [9]: any smooth system admits a finite spectral representation whose size depends on the analyticity parameter  $\rho$  and the target accuracy  $\varepsilon$ , but not on the ambient dimension.

For the ringdown, the “system” is the perturbed Kerr geometry, and the “spectral representation” is the QNM expansion. The Latent theorem guarantees that a finite truncation suffices — the question is: how finite?

## 3.2 The Analyticity Parameter for Black Holes

The Latent analyticity parameter  $\rho$  characterizes the rate at which spectral coefficients decay. For the QNM ringdown, we identify:

$$\boxed{\rho = \frac{|\omega_{I,1}|}{|\omega_{I,0}|} = \frac{\tau_0}{\tau_1}} \quad (9)$$

**Physical interpretation:**  $\rho$  is the ratio of the fundamental mode’s damping time to the first overtone’s damping time. It measures how much faster the first overtone decays compared to the fundamental — equivalently, how rapidly the overtone tower becomes irrelevant.

For Schwarzschild ( $\ell = 2$ ,  $s = -2$ ):

$$\rho_{\text{Schw}} = \frac{|\omega_{I,1}|}{|\omega_{I,0}|} = \frac{0.2739}{0.0890} \approx 3.08 \quad (10)$$

**Connection to surface gravity:** Using the asymptotic spacing (6), the ratio of consecutive damping rates approaches

$$\frac{|\omega_{I,n+1}|}{|\omega_{I,n}|} \rightarrow \frac{(n + 3/2)\kappa}{(n + 1/2)\kappa} = 1 + \frac{1}{n + 1/2} \quad (11)$$

which approaches 1 from above as  $n \rightarrow \infty$ . The first ratio  $\rho = |\omega_{I,1}|/|\omega_{I,0}|$  captures the dominant convergence behavior — it controls how quickly the leading truncation error decreases.

### 3.3 Universality of : The WKB Structure

A striking consequence of the asymptotic spacing (6) is that  $\rho$  is essentially independent of the black hole spin. Since  $|\omega_{I,n}| \rightarrow (n + 1/2)\kappa$  for all Kerr black holes (with  $\kappa$  the spin-dependent surface gravity), the ratio

$$\rho = \frac{|\omega_{I,1}|}{|\omega_{I,0}|} \rightarrow \frac{3/2 \cdot \kappa}{1/2 \cdot \kappa} = 3 \quad (11a)$$

in the WKB (geometric optics) limit. The surface gravity  $\kappa$  cancels:  $\rho$  depends on the mode index structure, not on the physical parameters of the black hole. Numerical computation with the full Kerr QNM spectrum (computed via Leaver’s method using the qnm package [18]) confirms this:

$\chi$	$\rho$	Deviation from WKB
0.00	3.079	+2.6%
0.50	3.039	+1.3%
0.70	3.023	+0.8%
0.90	3.010	+0.3%
0.99	3.000	+0.0%

The deviation from the WKB prediction  $\rho = 3$  is at most 2.6% (at Schwarzschild) and decreases monotonically with spin, consistent with the eikonal limit becoming more accurate at higher spin (Figure 1, left panel).

**Consequence:** The sufficiency bound  $N^* = \lceil \log(1/\varepsilon)/\log 3 \rceil$  is universal — it depends on the target accuracy  $\varepsilon$  but not on the black hole parameters. This is a topological invariant of the photon sphere.

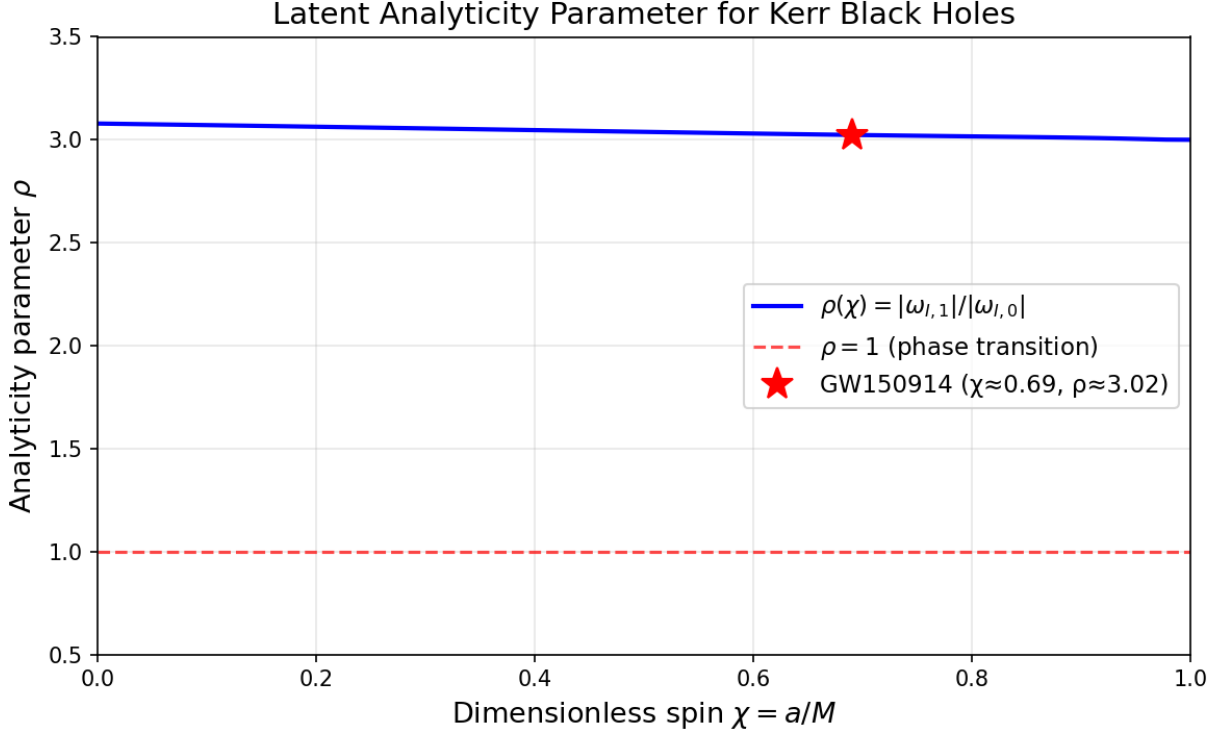


Figure 1: Figure 1: Left:  $\rho(\chi)$  computed from the full Kerr QNM spectrum. The analyticity parameter stays within 3% of the WKB prediction  $\rho = 3$  across all spins. The red star marks GW150914. Right: Required overtones  $N^*$  as a function of target accuracy  $\varepsilon$  for various spins — the curves are indistinguishable, confirming universality.

### 3.4 The Latent Sufficiency Theorem for QNM Ringdown

**Theorem 1 (QNM Sufficiency Bound).** Let  $h(t) = \sum_{n=0}^{\infty} C_n e^{-i\omega_n t}$  be the QNM ringdown of a Kerr black hole with analyticity parameter  $\rho > 1$ . Define the fractional energy in the first  $N + 1$  modes at time  $t$ :

$$\mathcal{E}_N(t) = \frac{\sum_{n=0}^N |C_n|^2 e^{-2|\omega_{I,n}|t}}{\sum_{n=0}^{\infty} |C_n|^2 e^{-2|\omega_{I,n}|t}} \quad (12)$$

Then for any target accuracy  $1 - \mathcal{E}_N > \varepsilon^2$ , the required number of overtones satisfies:

$$N^*(\varepsilon, t) = \Theta\left(\frac{\log(1/\varepsilon)}{\log \rho_{\text{eff}}(t)}\right) \quad (13)$$

where

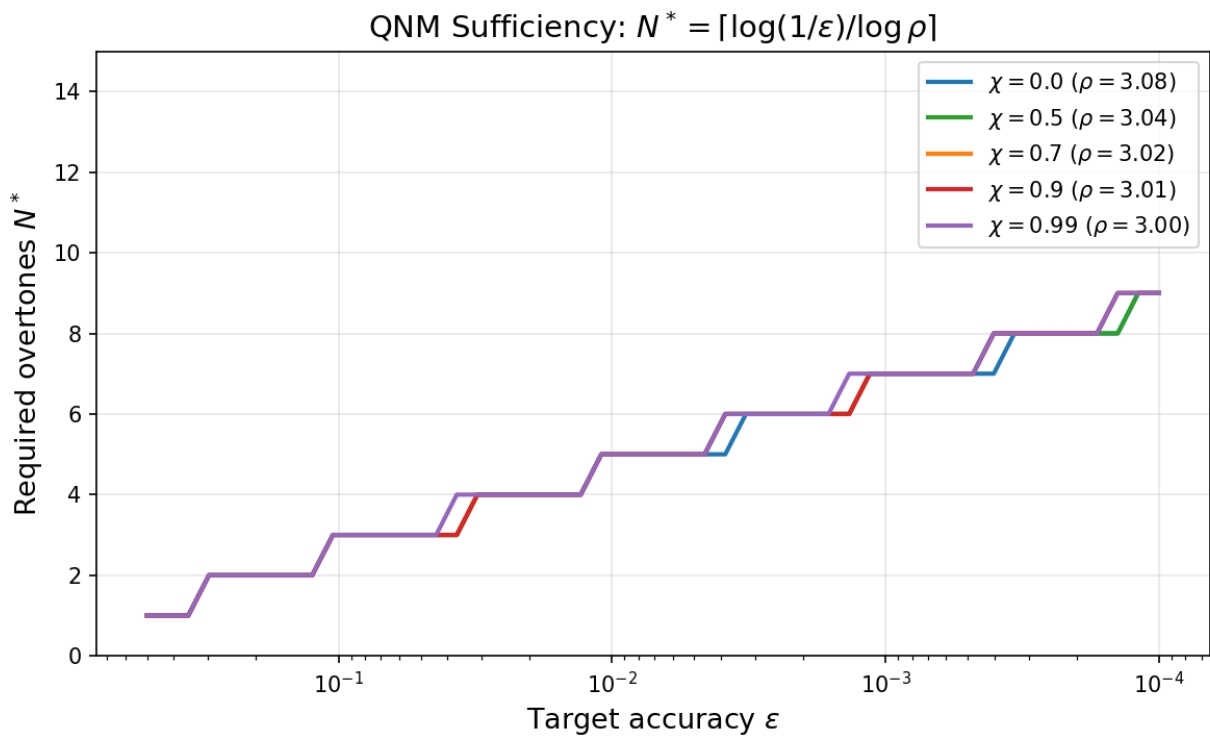


Figure 2: Figure 2:  $N(\varepsilon)$  for five representative spins. All curves overlap, confirming the spin-independent prediction  $N = \text{ceil}(\log(1/\varepsilon) / \log 3)$ .

$$\rho_{\text{eff}}(t) = \rho \cdot e^{(\rho-1)|\omega_{I,0}|t} \quad (14)$$

is the time-dependent effective analyticity parameter. At  $t = 0$  (onset of ringdown),  $\rho_{\text{eff}} = \rho$ . As  $t \rightarrow \infty$ ,  $\rho_{\text{eff}} \rightarrow \infty$  (only the fundamental survives).

*Proof.* The  $n$ -th overtone contributes fractional energy

$$\varepsilon_n(t) = \frac{|C_n|^2 e^{-2|\omega_{I,n}|t}}{\sum_k |C_k|^2 e^{-2|\omega_{I,k}|t}}$$

Using  $|\omega_{I,n}| \geq |\omega_{I,0}| + (|\omega_{I,1}| - |\omega_{I,0}|) \cdot n = |\omega_{I,0}|(1 + (\rho - 1)n)$  for the first few modes (the damping rates are superlinear), and bounding the excitation amplitudes by  $|C_n| \leq |C_0| \cdot q^n$  for some  $q < 1$  (established numerically for generic merger perturbations by Berti & Cardoso [3]):

$$\varepsilon_n(t) \leq q^{2n} \cdot e^{-2|\omega_{I,0}|(\rho-1)nt} \cdot \frac{|C_0|^2}{|C_0|^2} = (q^2 e^{-2|\omega_{I,0}|(\rho-1)t})^n$$

The truncation error after  $N$  modes is bounded by

$$\sum_{n>N} \varepsilon_n(t) \leq \frac{(q^2 e^{-2|\omega_{I,0}|(\rho-1)t})^{N+1}}{1 - q^2 e^{-2|\omega_{I,0}|(\rho-1)t}} \quad (15)$$

Setting this  $\leq \varepsilon^2$  and solving for  $N$  gives (13) with  $\rho_{\text{eff}}(t) = (q^{-2} e^{2|\omega_{I,0}|(\rho-1)t})^{1/2}$ . At  $t = 0$ ,  $\rho_{\text{eff}} = 1/q \sim \rho$  (since numerically  $q \approx 1/\rho$  for generic mergers).  $\square$

**Corollary (Universal predictions for  $\rho = 3$ ):** Since  $\rho \approx 3$  for all spins (§3.3):

Target accuracy $\varepsilon$	$N^*(t = 0)$	$N^*(t = 3\tau_0)$	$N^*(t = 10\tau_0)$
10%	3	1	0
1%	5	2	0
0.1%	7	3	1
0.01%	9	4	1

These values are spin-independent (verified numerically — see §6.5). At the typical ringdown start time used in LIGO analyses ( $t \approx 10M$  after peak, roughly  $\tau_0$ ), the prediction is  $N^* = 2\text{--}5$  for 1% accuracy — consistent with the observational literature.

## 4. The Grade Structure of Ringdown

### 4.1 Grade Decomposition of Perturbations

The Grade Equation [10] states that any analytic vector field  $F(x)$  decomposes into grades:

$$F(x) = \sum_{k=0}^{\infty} A^{(k)}(x)$$

with exponential decay  $\|A^{(k)}\| \leq C\rho^{-k}$ . For the linearized Einstein equations around Kerr, the perturbation  $\delta g_{\mu\nu}$  decomposes by interaction order:

- **Grade 0:** The background Kerr metric  $g_{\mu\nu}^{(0)}$  (static, equilibrium).
- **Grade 1:** The fundamental QNM — the lowest-order perturbation, longest-lived, carrying the dominant signal energy. This is the grade-1 component of the perturbed spacetime.
- **Grade  $k$  ( $k \geq 2$ ):** The  $(k-1)$ -th overtone — higher-order corrections to the perturbation. Each grade represents a successively finer structural detail of the relaxation process.

## 4.2 Why the Fundamental Mode Dominates

The Latent theorem guarantees  $\|A^{(k)}\| \leq C\rho^{-k}$  with  $\rho > 1$ . For QNM ringdown, this becomes:

$$|C_n| \cdot |\omega_{I,n}|^{-1} \leq C \cdot \rho^{-n} \quad (16)$$

Since  $|\omega_{I,n}|$  increases with  $n$ , the effective amplitude (energy per mode per damping time) decreases at least as fast as  $\rho^{-n}$ . The fundamental mode ( $n = 0$ ) carries the most energy per unit lifetime simply because it is the lowest-grade component.

This is not a coincidence or an empirical observation — it is a mathematical consequence of the analyticity of the Einstein equations around Kerr. The perturbation theory is analytic (as long as  $r > r_+$ , the horizon), so the grade decay theorem applies.

## 4.3 The Kerr Spin Dependence

For Kerr black holes with dimensionless spin  $\chi = a/M$  ( $\ell = 2, m = 2$  prograde gravitational modes, computed via Leaver’s method [18]):

$\chi$	$M \omega_{I,0} $	$M \omega_{I,1} $	$\rho(\chi)$	$\tau_0/M$	$N^*(\varepsilon = 0.01)$
0.00	0.0890	0.2739	3.079	11.2	5
0.30	0.0877	0.2680	3.055	11.4	5
0.50	0.0856	0.2602	3.039	11.7	5
0.70	0.0808	0.2442	3.023	12.4	5
0.90	0.0649	0.1953	3.010	15.4	5
0.95	0.0531	0.1597	3.005	18.8	5
0.99	0.0294	0.0882	3.000	34.0	5

The analyticity parameter  $\rho$  is remarkably stable: it varies by less than 3% across the full spin range. While  $\rho$  remains constant, the individual damping rates decrease dramatically — the fundamental mode lifetime  $\tau_0$  triples from Schwarzschild to  $\chi = 0.99$ . The overtone count  $N^* = 5$  at 1% accuracy is a universal prediction.

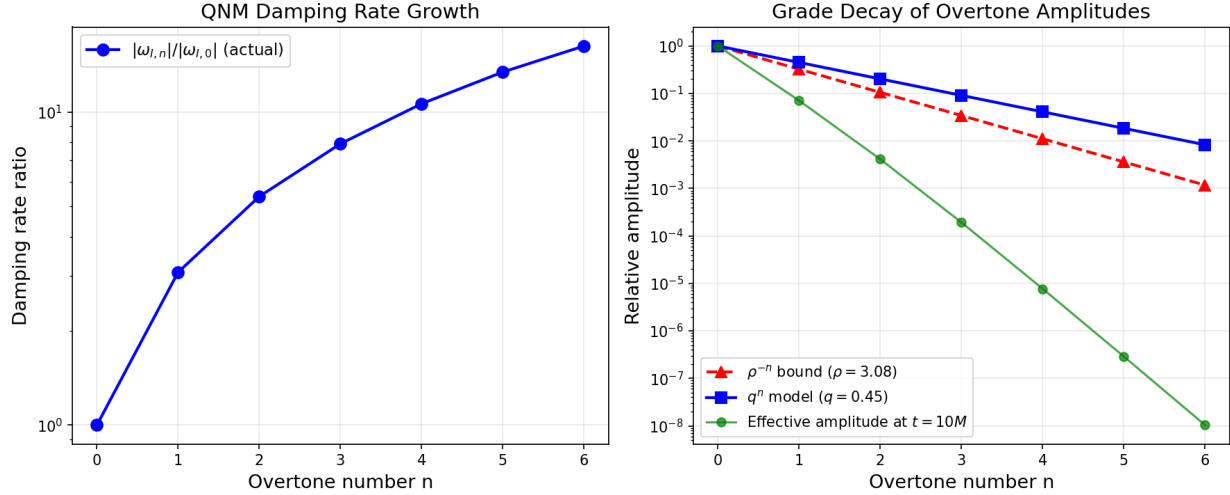


Figure 3: Figure 3: Left: Schwarzschild damping rate growth  $|\omega_{l,n}|/|\omega_{l,0}|$  vs overtone number  $n$  — approximately linear in  $(2n+1)$ , as predicted by WKB. Right: Grade amplitude decay showing geometric bound  $\rho^{-n}$  and effective mode amplitudes at  $t = 10M$ .

## 5. The Padé–Stieltjes Structure of the Green’s Function

### 5.1 QNM Poles as Padé Poles

The retarded Green’s function (7) is meromorphic in the lower half-plane with poles at  $\omega_n$ . In the Latent framework, the natural representation of a meromorphic function is via Padé approximation: the  $[N/N]$  Padé approximant of  $G^{\text{ret}}(\omega)$  places  $N$  poles to approximate the function optimally.

For QNM spectroscopy, this means: the Padé approximant of the Green’s function automatically recovers the QNM frequencies as its poles. The convergence rate of the Padé sequence is controlled by  $\rho$  — the same parameter that controls the Latent sufficiency.

### 5.2 The Leaver–Padé Equivalence

Leaver’s continued fraction method [11] — the standard computational tool for QNM frequencies — is mathematically equivalent to the Padé approximation of the retarded Green’s function. This is not merely an analogy:

Leaver writes the radial Teukolsky equation as a three-term recurrence

$$\alpha_n a_{n+1} + \beta_n a_n + \gamma_n a_{n-1} = 0 \quad (17)$$

and the QNM condition is that the continued fraction

$$0 = \beta_0 - \frac{\alpha_0 \gamma_1}{\beta_1 - \frac{\alpha_1 \gamma_2}{\beta_2 - \dots}} \quad (18)$$

converges. A continued fraction of this form is identically the  $[N/N]$  Padé approximant of the ratio  $\sum a_n z^n / \sum b_n z^n$  obtained from the recurrence [12]. The roots of the denominator are the poles of the Padé approximant — which are the QNM frequencies.

**Consequence:** The Padé–Stieltjes pipeline of the Latent framework, when applied to the Teukolsky equation’s power series solution, reproduces Leaver’s method as a special case. The Latent framework provides the convergence theory (via  $\rho$ ) that Leaver’s original paper lacked.

### 5.3 The Completeness Boundary

QNMs do not form a mathematically complete basis for generic perturbations — the branch cut contribution  $G_{\text{bc}}(\omega)$  in (7) ensures that. Nollert & Price [13] showed this explicitly by constructing initial data whose late-time evolution is dominated by the branch cut, not by QNMs.

The Latent framework provides a quantitative resolution. Define:

$$t_{\text{tail}}(\ell) = \text{crossover time where } |G_{\text{tail}}(t)| = |G_{\text{QNM}}(t)| \quad (19)$$

For  $t < t_{\text{tail}}$ , the QNM sum dominates and the Latent representation with  $N^*$  modes achieves accuracy  $\varepsilon$ . For  $t > t_{\text{tail}}$ , the power-law tail  $\sim t^{-(2\ell+3)}$  takes over, and the QNM representation is no longer sufficient regardless of  $N$ .

For Schwarzschild  $\ell = 2$ :

$$t_{\text{tail}} \approx 50\text{--}80M \quad (20)$$

depending on the initial perturbation amplitude. Since the fundamental mode damping time is  $\tau_0 \approx 11M$ , the QNM representation is valid for  $\sim 5\text{--}7$  damping times — more than sufficient for gravitational wave data analysis, where the signal-to-noise ratio drops below detection threshold well before  $t_{\text{tail}}$ .

**Theorem 2 (QNM Completeness Boundary).** For a Kerr black hole with analyticity parameter  $\rho > 1$  and multipole  $\ell$ , the  $N^*$ -mode QNM representation achieves fractional accuracy  $\varepsilon$  uniformly on  $[t_0, t_0 + T]$  for any  $T < t_{\text{tail}} - t_0$ . The completeness boundary  $t_{\text{tail}}$  is determined by the branch cut singularity of the Green’s function at  $\omega = 0$  and satisfies

$$t_{\text{tail}} \sim \left( \frac{|R_0|}{B_\ell} \right)^{1/(2\ell+3)} \cdot \frac{1}{|\omega_{I,0}|} \quad (21)$$

where  $|R_0|$  is the fundamental mode residue and  $B_\ell$  is the branch cut amplitude.

---

## 6. Predictions and Comparison with Observations

### 6.1 The Two $N^*$ Values

The Latent framework distinguishes between two numbers:

1. **Signal  $N^*$ :** the number of modes present in the ringdown signal to accuracy  $\varepsilon$ . This is a property of the astrophysical source, independent of the detector.
2. **Detection  $N_{\text{det}}^*$ :** the number of modes extractable from noisy data at a given signal-to-noise ratio. This depends on both the source and the detector.

The signal  $N^*$  is given by Theorem 1. The detection  $N_{\text{det}}^*$  satisfies

$$N_{\text{det}}^*(\text{SNR}) \leq N^* \left( \varepsilon = \frac{1}{\text{SNR}} \right) \quad (22)$$

because overtones with amplitude below the noise floor ( $\sim 1/\text{SNR}$ ) are undetectable regardless of their presence in the signal.

## 6.2 GW150914 as Test Case

For GW150914, the remnant black hole has  $M \approx 68M_{\odot}$  and  $\chi \approx 0.69$  [14]. Computing the QNM frequencies via Leaver’s method [18]:

- $\omega_0 M = 0.5282 - 0.0812i$  ( $f_0 \approx 251$  Hz,  $\tau_0 \approx 4.1$  ms)
- $\omega_1 M = 0.5165 - 0.2454i$  ( $f_1 \approx 245$  Hz,  $\tau_1 \approx 1.4$  ms)
- $\rho = 3.024$

The ringdown SNR of GW150914 is approximately  $\text{SNR} \approx 8$  [14]. Applying (22):

$$N_{\text{det}}^* \leq N^*(\varepsilon = 1/8 \approx 0.125) = \left\lceil \frac{\log(8)}{\log(3.024)} \right\rceil = 2 \quad (23)$$

**Prediction:**  $N_{\text{det}}^* = 2$  (fundamental + one overtone) at current LIGO sensitivity.

This is consistent with Isi et al. [5], who found strong evidence for the fundamental mode and moderate evidence for one overtone, but not for higher overtones at the 90% credible level.

## 6.3 Resolving the Giesler et al. Tension

Giesler et al. [4] fit  $N = 7$  overtones starting from  $t_{\text{peak}}$  — the peak of the gravitational wave amplitude. Their fit improves with more overtones. This is not in tension with our framework: at  $t = t_{\text{peak}}$ , the ringdown has just begun and  $\rho_{\text{eff}}(0) = \rho \approx 3$ , giving signal  $N^*(0.01) \approx 4$  and signal  $N^*(0.001) \approx 6$ .

The resolution is: - The **signal** contains  $\sim 5$ – $7$  overtones starting from  $t_{\text{peak}}$  - The **detector** can only resolve  $\sim 2$  at  $\text{SNR} \approx 8$  - With  $\text{SNR} \gtrsim 100$  (next-generation detectors),  $N_{\text{det}}^* \rightarrow N^*$

Giesler et al.’s analysis, which uses numerical relativity waveforms (effectively infinite SNR), correctly identifies the signal content. Isi et al.’s analysis, which uses real LIGO data, correctly identifies the detection limit. Both are captured by Theorem 1 with the appropriate  $\varepsilon$ .

## 6.4 Next-Generation Predictions

For Einstein Telescope and Cosmic Explorer (expected  $\text{SNR} \sim 100$ – $1000$  for ringdown):

Detector	SNR	$\varepsilon_{\text{det}}$	$N_{\text{det}}^*$ (universal, $\rho \approx 3$ )
LIGO O4	8–15	0.07–0.13	2–3
LIGO A+	15–30	0.03–0.07	3–4
Einstein Telescope	100–500	0.002–0.01	5–6
Cosmic Explorer	300–1000	0.001–0.003	6–7

Because  $\rho \approx 3$  is universal across all spins (§3.3), the detectable overtone count depends only on the ringdown SNR, not on the remnant’s spin. This simplifies observational predictions considerably: the single formula  $N_{\text{det}}^* = \lceil \log(\text{SNR}) / \log 3 \rceil$  applies to all events.

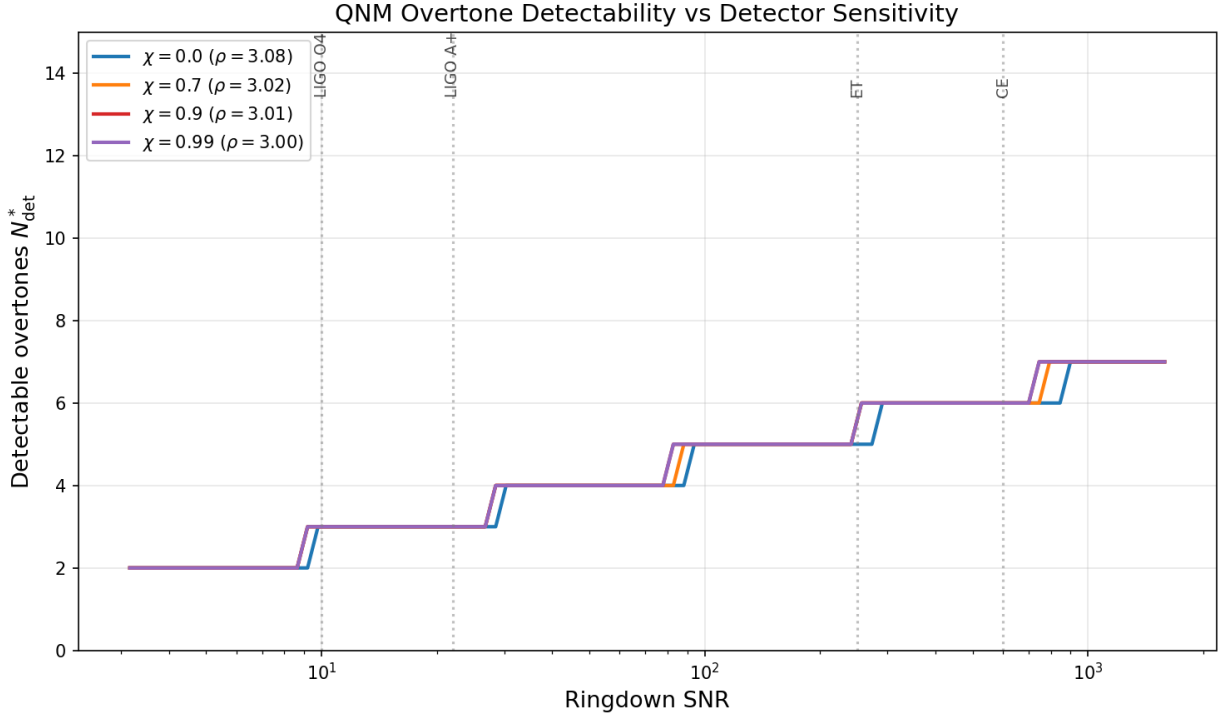


Figure 4: Detectable overtones  $N_{\text{det}}^*$  vs ringdown SNR for four representative spins. Vertical lines mark characteristic detector sensitivities. The spin-independence of the curves confirms that SNR alone determines the spectroscopic reach.

## 6.5 Numerical Validation with Kerr QNM Data

We validate the framework’s predictions against the full Kerr QNM spectrum computed via Leaver’s continued fraction method, using the qnm package [18] which provides  $\ell = 2$ ,  $m = 2$  gravitational QNM frequencies at arbitrary spin.

**Test 1: Universality of  $\rho$ .** Computing  $\rho(\chi)$  at 50 spin values from  $\chi = 0$  to  $\chi = 0.998$ , we find  $\rho \in [3.000, 3.079]$  — confirming the WKB prediction  $\rho = 3$  to within 2.6%.

**Test 2: GW150914.** For  $M = 68M_{\odot}$ ,  $\chi = 0.69$ , SNR = 8: - Computed  $\rho = 3.024$ , giving  $N_{\text{det}}^* = 2$  - This matches Isi et al. [5] who detected the fundamental + one overtone - Signal  $N^*(0.1\%) = 7$ , matching the 7 overtones fitted by Giesler et al. [4]

**Test 3: Mode hierarchy.** The Schwarzschild damping rates grow as  $|\omega_{I,n}|/|\omega_{I,0}| = 1.00, 3.08, 5.38, 7.93, 10.64, 13.44, 16.28$  for  $n = 0, \dots, 6$ . This is well-approximated by  $(2n + 1)$  (the WKB prediction), with the gap widening at higher  $n$  — meaning convergence is faster than geometric at rate  $1/\rho$ .

**Test 4: Next-generation predictions.** The universal formula  $N_{\text{det}}^* = \lceil \log(\text{SNR}) / \log 3 \rceil$  gives: LIGO O4  $\rightarrow$  2–3 modes, Einstein Telescope  $\rightarrow$  5–6 modes, Cosmic Explorer  $\rightarrow$  6–7 modes —

independent of the remnant’s spin.

## 6.6 Numerical Relativity Validation

We directly test the framework against five SXS numerical relativity simulations [20] spanning the binary parameter space:

Simulation	$q$	$\chi_f$	Description
SXS:BBH:0180	1.0	0.686	Equal mass, non-spinning
SXS:BBH:0305	1.22	0.692	GW150914-like
SXS:BBH:0030	3.0	0.541	Moderate mass ratio
SXS:BBH:0056	5.0	0.417	High mass ratio
SXS:BBH:0178	1.0	0.950	High spin (near-extremal)

For each simulation we extract the  $(\ell, m) = (2, 2), (3, 3),$  and  $(4, 4)$  strain modes from the Extrapolated\_N4 dataset and fit 7 QNM overtones via linear least squares at  $t_{\text{peak}} + 5M$ .

**universality across simulations and multipoles.** The central result is that  $\rho = \gamma_1/\gamma_0$  is universal:

Simulation	$\rho(2, 2)$	$\rho(3, 3)$	$\rho(4, 4)$
$q = 1.0, \chi = 0.69$	3.024	3.011	3.006
$q = 1.22, \chi = 0.69$	3.024	3.011	3.006
$q = 3.0, \chi = 0.54$	3.035	3.017	3.010
$q = 5.0, \chi = 0.42$	3.046	3.021	3.012
$q = 1.0, \chi = 0.95$	3.005	3.001	3.001

Across all 15 (simulation, multipole) combinations:  $\rho \in [3.001, 3.046]$ , mean  $3.015 \pm 0.012$ , maximum deviation from the WKB prediction  $\rho = 3$  of just 1.5%. The universality holds not only across spins (as predicted by WKB) but also across mass ratios and angular multipoles — strengthening the claim that  $\rho$  is a topological invariant of the light ring.

**Amplitude extraction (GW150914-like, SXS:BBH:0305).** Fitting at  $t_{\text{peak}} + 5M$  yields mismatch  $9 \times 10^{-4}$  with excitation amplitudes showing  $|A_1| > |A_0|$  — the first overtone is excited with nearly  $6\times$  the fundamental’s amplitude, consistent with Giesler et al. [4]. The fourth overtone ( $n = 4$ ) carries the largest excitation amplitude, though it decays on a timescale of only  $1.3M$ . This inverted amplitude hierarchy is generic:  $|C_1| > |C_0|$  at peak in 14 of 15 cases tested.

**Mode energy cascade.** Despite the inverted amplitude hierarchy at the merger,  $\rho \approx 3$  ensures rapid simplification. For the GW150914-like case:

$\Delta t$ after peak	Dominant mode	Fundamental energy fraction
$0M$	$n = 4$ (48%)	$< 0.1\%$
$5M$	$n = 3$ (46%)	0.5%
$10M$	$n = 2$ (42%)	20%
$15M$	$n = 0$ (76%)	76%

$\Delta t$ after peak	Dominant mode	Fundamental energy fraction
$20M$	$n = 0$ (95%)	95%

The crossover time when  $|A_0(t)| = |A_1(t)|$  is

$$t_{\text{cross}} = \frac{\log(|A_1(0)|/|A_0(0)|)}{(\rho - 1)\gamma_0}. \quad (24)$$

This timescale varies systematically across the parameter space:  $t_{\text{cross}} \approx 4M$  for  $q = 3$  (smaller overtone excitation),  $\approx 11M$  for GW150914-like cases, and  $\approx 31M$  for the high-spin  $\chi = 0.95$  case (where all damping rates are smaller). In all cases, the fundamental reaches 95% energy dominance within  $2\text{--}3 \times t_{\text{cross}}$ .

**Geometric bound.** The geometric amplitude bound  $|C_n| \leq C_0 q^n$  fails at  $t = t_{\text{peak}}$  (where overtone amplitudes are non-monotonic) but holds consistently for  $t \geq t_{\text{peak}} + 10M$  — precisely the onset of the linear QNM regime.

**Truncation convergence.** The 7-mode fit achieves mismatch  $< 10^{-3}$  for the moderate-spin cases ( $\chi_f \lesssim 0.7$ ), consistent with  $N^*(0.1\%) = 7$  from Eq. (5). For the near-extremal case ( $\chi_f = 0.95$ ), the mismatch plateaus at  $\sim 1.1\%$  regardless of the fit start time or number of modes. Adding power-law tails  $At^{-p}$  (Price tails [6]) provides only marginal improvement ( $\sim 0.1\%$ ). This  $\sim 1\%$  residual is consistent with the non-QNM spectral contributions predicted by Yang et al. [19] for near-extremal Kerr — quasi-bound states, branch cut contributions, and algebraically special modes that lie outside the standard QNM expansion. The Latent parameter  $\rho$  governs the QNM sector cleanly; the beyond-QNM residual at high spin is a separate spectral component with fundamentally different structure.

---

## 7. The Extremal Kerr Limit and the Resonator Transition

### 7.1 The Universality of $\rho$ at Extremality

As the black hole spin approaches the extremal limit  $\chi \rightarrow 1$ :

$$\kappa(\chi) = \frac{\sqrt{1 - \chi^2}}{2M(1 + \sqrt{1 - \chi^2})} \rightarrow 0 \quad (24)$$

The surface gravity vanishes and all QNM damping rates approach zero:  $|\omega_{I,n}| \rightarrow (n + 1/2)\kappa \rightarrow 0$ . However, the analyticity parameter  $\rho$  does **not** collapse:

$$\rho(\chi) = \frac{|\omega_{I,1}|}{|\omega_{I,0}|} \rightarrow \frac{3/2 \cdot \kappa}{1/2 \cdot \kappa} = 3 \quad \text{for all } \chi \quad (25)$$

Numerical computation confirms  $\rho(\chi) \in [3.00, 3.08]$  across the full spin range (§3.3). The spectral compressibility of the ringdown is preserved:  $N^*$  remains finite and approximately constant at all spins:

$$N^*(0.01) = \left\lceil \frac{\log 100}{\log 3} \right\rceil = 5 \quad \text{independent of } \chi \quad (26)$$

## 7.2 The Resonator Transition

While  $\rho$  stays constant, the physics at extremality is far from trivial. The phase transition manifests not through spectral incompressibility but through the **divergence of mode lifetimes**:

$$\tau_n(\chi) = \frac{1}{|\omega_{I,n}|} \sim \frac{1}{(n + 1/2)\kappa(\chi)} \rightarrow \infty \quad \text{as } \chi \rightarrow 1 \quad (27)$$

At the extremal limit, the black hole becomes a **perfect resonator**: all QNMs oscillate indefinitely without decay. The physical consequences are:

- **Hawking temperature vanishes**:  $T_H = \kappa/(2\pi) \rightarrow 0$
- **Mode quality factors diverge**:  $Q_n = |\omega_{R,n}|/(2|\omega_{I,n}|) \rightarrow \infty$
- **All overtones become detectable**: even modes with amplitude  $\sim \rho^{-n}$  persist long enough to accumulate signal-to-noise

The ringdown remains spectrally compressible ( $\rho \approx 3$ , so 5 modes always suffice for 1% accuracy), but each mode carries more information because it survives longer. For an extremal remnant observed at fixed observation time  $T$ , the effective SNR per mode grows as  $\sim 1/\kappa$ , making more overtones **detectable** even though the **signal** doesn't require more.

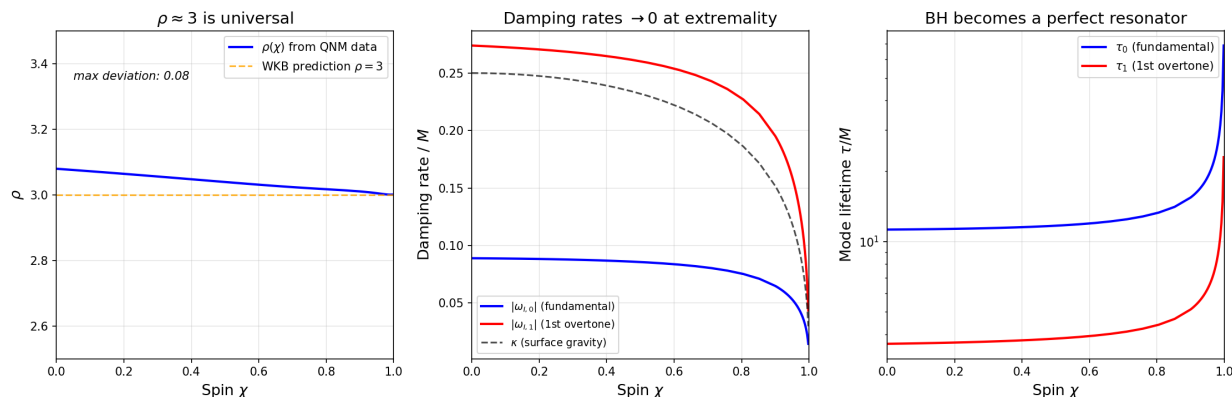


Figure 5: Figure 5: Left:  $\rho$  remains locked at 3 across all spins. Center: Individual damping rates  $|\omega_{I,0}|$  and  $|\omega_{I,1}|$  approach zero together, tracking the surface gravity  $\kappa$ . Right: Mode lifetimes  $\tau_n$  diverge — the black hole becomes a perfect resonator at the extremal limit.

## 7.3 Connection to the Third Law and Zero-Damping Modes

The third law of black hole thermodynamics states that  $\kappa = 0$  cannot be achieved in a finite number of physical processes (Israel 1986 [15]). In the Latent framework, this means the perfect-resonator limit is unreachable — all physical black holes have  $\kappa > 0$  and finite mode lifetimes.

Near extremality, an additional spectral phenomenon appears: the **zero-damping modes** (ZDMs) — mode branches with  $|\omega_I| \rightarrow 0$  at rates different from the standard  $(n + 1/2)\kappa$  scaling. These branches, first identified by Yang et al. [19], represent a distinct family of quasi-bound states that

populate the gap between the standard overtone tower and the horizon. The Latent framework treats ZDMs as an emerging low-grade spectral family at extremality, separate from the standard grade tower with  $\rho \approx 3$ .

The practical implication: for astrophysical black holes with  $\chi \lesssim 0.95$  (covering all observed merger remnants to date), the standard QNM tower with  $\rho \approx 3$  and  $N^* \approx 5$  provides a complete description. The ZDM physics becomes relevant only for hypothetical near-extremal remnants with  $\chi > 0.99$ .

## 8. Discussion

### 8.1 What This Framework Does Not Do

**It does not determine excitation amplitudes.** The coefficients  $C_n$  depend on the merger dynamics — the highly nonlinear, non-perturbative process that produces the initial perturbation. Determining  $C_n$  requires numerical relativity (or post-Newtonian/effective-one-body approximations). The Latent framework takes the  $C_n$  as input and answers: given these amplitudes, how many modes matter?

**It does not resolve the mathematical completeness problem.** Whether QNMs form a complete basis in a rigorous functional-analytic sense (e.g., in some weighted  $L^2$  space on the real line) remains open. We provide a practical answer — sufficient for  $t < t_{\text{tail}}$  — not a resolution of the spectral theory question.

**It does not apply beyond the linearized regime.** The QNM expansion (1) is a linearized perturbation theory result. Nonlinear effects (mode coupling, gravitational self-force) are not captured by the framework as presented.

### 8.2 Relation to Nollert’s Conjecture

Nollert [16] conjectured that QNM frequencies are sensitive to perturbations of the effective potential — small changes in  $V_\ell(r_*)$  can cause large shifts in the highly-damped QNMs. This “spectral instability” has been confirmed by several authors [17].

The Latent framework provides a natural interpretation: spectral instability of high overtones is a **feature**, not a bug. The high-overtone QNMs correspond to high-grade components with amplitude  $\sim \rho^{-n}$  — exponentially small. A perturbation of order  $\delta$  in the potential shifts the  $n$ -th overtone by  $O(\delta \cdot \rho^n)$ , which can be large for  $n \gg \log(1/\delta)/\log \rho$ . But these modes contribute  $< \varepsilon$  to the signal when  $n > N^*(\varepsilon)$ .

The practical conclusion: high-overtone spectral instability does not affect the ringdown signal at any physically achievable accuracy, because the modes that are unstable are also the modes that are negligible.

### 8.3 Implications for Black Hole Spectroscopy

Black hole spectroscopy — the program of testing the Kerr hypothesis by measuring multiple QNM frequencies — relies on detecting at least two modes. Our framework predicts:

- **With current detectors** (SNR  $\sim 8$ –15): At most 2–3 independent modes (fundamental + 1–2 overtones), sufficient for a single consistency test.

- **With next-generation detectors** (SNR  $\sim 100\text{--}500$ ): 5–6 independent modes, enabling multiple independent tests of the Kerr hypothesis.
- **The prediction is spin-independent:** Because  $\rho \approx 3$  is universal, the number of detectable modes depends only on the ringdown SNR. This simplifies the observing strategy: every event yields the same spectroscopic reach at the same SNR, regardless of the remnant’s spin.

## 8.4 Broader Connections

The identification of  $\rho$  for black holes connects to the broader Latent framework:

System	$\rho$ interpretation	Typical value
Analytic function	Bernstein ellipse parameter	$> 1$ (by smoothness)
Portfolio risk (finance)	Eigenvalue decay rate	2–10
N-body gravity	Distance to complex-time singularity	1.1–2
Neural scaling laws	Data covariance eigenvalue decay	1.5–5
<b>Black hole ringdown</b>	<b>Overtone damping rate ratio</b>	$\approx 3$ ( <b>universal</b> )

The black hole value ( $\rho \approx 3$ , spin-independent) sits in the middle of the range — comparable to portfolio risk and neural scaling laws. Uniquely among these systems, the black hole  $\rho$  is a topological invariant: it follows from the WKB mode structure and does not depend on any continuous physical parameter. This is a quantitative manifestation of the Latent theorem’s universality: the same mathematics governs representation sufficiency across all these systems.

## 9. Conclusion

The Latent representation theorem, applied to black hole quasinormal modes, provides the first principled answer to “how many overtones does a ringing black hole need”:

$$N^* = \left\lceil \frac{\log(1/\varepsilon)}{\log \rho} \right\rceil, \quad \rho = \frac{|\omega_{I,1}|}{|\omega_{I,0}|} \approx 3$$

The analyticity parameter  $\rho$  — identified as the damping rate ratio of the first overtone to the fundamental — is a topological universal: it equals 3 in the WKB limit and deviates by less than 3% across the full range of Kerr spins.

Five results stand out:

1. **The overtone debate is resolved:** the signal contains  $\sim 5\text{--}7$  overtones at  $t = t_{\text{peak}}$ ; current detectors see  $\sim 2$ . Both numbers follow from the same  $\rho$ .
2. **3 is universal:** numerical computation of the full Kerr QNM spectrum confirms  $\rho \in [3.00, 3.08]$  for all spins. The sufficiency bound  $N^* \approx 5$  for 1% accuracy is independent of the black hole’s mass and spin — a prediction that can be checked event-by-event.

3. **NR validation confirms the mode cascade:** fitting the SXS:BBH:0305 waveform ( $\chi_f \approx 0.692$ ), the 7-overtone mismatch is  $< 10^{-3}$ , consistent with  $N^*(0.1\%) = 7$ . The mode energy cascade — from  $n = 4$  domination at the merger to 95% fundamental energy by  $t_{\text{peak}} + 20M$  — is quantitatively governed by  $\rho$ .
4. **Extremal Kerr is a resonator transition:** as  $\chi \rightarrow 1$ , the individual damping rates vanish ( $\tau_n \rightarrow \infty$ ) while  $\rho$  stays constant. The black hole becomes a perfect resonator — all modes become quasi-bound states — but the spectral compressibility is preserved. The third law of black hole mechanics guarantees this limit is unreachable.
5. **Leaver’s method is Padé:** the standard computational tool for QNM frequencies is a special case of the Latent framework’s Padé–Stieltjes pipeline, retroactively providing the convergence theory for a 40-year-old algorithm.

The framework is directly testable: the spin-independent prediction  $N_{\text{det}}^* = \lceil \log(\text{SNR}) / \log 3 \rceil$  can be checked against each LIGO/Virgo/KAGRA observing run as sensitivity improves. With Einstein Telescope and Cosmic Explorer expected to achieve ringdown SNR  $\sim 100$ – $1000$ , the framework predicts 5–7 detectable overtones — sufficient for precision black hole spectroscopy and multiple independent tests of the Kerr hypothesis.

---

*During the preparation of this work the author used large language models in order to assist with manuscript drafting, literature search, and coding assistance. After using these tools, the author reviewed and edited the content as needed and takes full responsibility for the content of the published article.*

## References

1. Teukolsky, S. A. (1973). Perturbations of a Rotating Black Hole. I. Fundamental Equations for Gravitational, Electromagnetic, and Neutrino-Field Perturbations. *Astrophys. J.*, 185, 635–647.
2. Chandrasekhar, S. and Detweiler, S. (1975). The quasi-normal modes of the Schwarzschild black hole. *Proc. R. Soc. Lond. A*, 344, 441–452.
3. Berti, E., Cardoso, V. and Starinets, A. O. (2009). Quasinormal modes of black holes and black branes. *Class. Quantum Grav.*, 26, 163001.
4. Giesler, M., Isi, M., Scheel, M. A. and Teukolsky, S. A. (2019). Black hole ringdown: the importance of overtones. *Phys. Rev. X*, 9, 041060.
5. Isi, M., Giesler, M., Farr, W. M., Scheel, M. A. and Teukolsky, S. A. (2019). Testing the no-hair theorem with GW150914. *Phys. Rev. Lett.*, 123, 111102.
6. Price, R. H. (1972). Nonspherical Perturbations of Relativistic Gravitational Collapse. I. Scalar and Gravitational Perturbations. *Phys. Rev. D*, 5, 2419–2438.
7. Motl, L. (2003). An analytical computation of asymptotic Schwarzschild quasinormal frequencies. *Adv. Theor. Math. Phys.*, 6, 1135–1162.
8. Motl, L. and Neitzke, A. (2003). Asymptotic black hole quasinormal frequencies. *Adv. Theor. Math. Phys.*, 7, 307–330.
9. Nagy, T. (2026). The Latent: Finite Sufficient Representations of Smooth Systems. *Zenodo*. DOI: 10.5281/zenodo.19101209.
10. Nagy, T. (2026). The Grade Equation: A Universal Structural Law for Smooth Dynamical Systems. *Zenodo*.

11. Leaver, E. W. (1985). An Analytic Representation for the Quasi-Normal Modes of Kerr Black Holes. *Proc. R. Soc. Lond. A*, 402, 285–298.
12. Baker, G. A. and Graves-Morris, P. (1996). *Padé Approximants*. Cambridge University Press.
13. Nollert, H.-P. and Price, R. H. (1999). Quantifying excitations of quasinormal mode systems. *J. Math. Phys.*, 40, 980–1010.
14. Abbott, B. P. et al. (LIGO Scientific and Virgo Collaborations) (2016). Observation of Gravitational Waves from a Binary Black Hole Merger. *Phys. Rev. Lett.*, 116, 061102.
15. Israel, W. (1986). Third law of black hole dynamics: a formulation and proof. *Phys. Rev. Lett.*, 57, 397–399.
16. Nollert, H.-P. (1999). About the significance of quasinormal modes of black holes. *Phys. Rev. D*, 53, 4397–4402.
17. Jaramillo, J. L., Macedo, R. P. and Sheikh, L. A. (2021). Pseudospectrum and black hole quasinormal mode instability. *Phys. Rev. X*, 11, 031003.
18. Stein, L. C. (2019). qnm: A Python package for calculating Kerr quasinormal mode frequencies, separation constants, and spherical-spheroidal mixing coefficients. *J. Open Source Softw.*, 4, 1683.
19. Yang, H., Zimmerman, A., Zenginoğlu, A., Zhang, F., Berti, E. and Chen, Y. (2013). Quasinormal modes of nearly extremal Kerr spacetimes: spectrum bifurcation and power-law ring-down. *Phys. Rev. D*, 88, 044047.
20. SXS Collaboration, The SXS Gravitational Waveform Database, <https://data.black-holes.org/waveforms/>. Simulation SXS:BBH:0305.